PERIÓDICO TCHÊ QUÍMICA
ARTIGO ORIGINAL

O COMPOSTO QUATERNÁRIO DE CALCOGENIDA $Ag_2FeGeSe_4$: UMA REVISÃO DE SUA ESTRUTURA CRISTAL E PROPRIEDADES MAGNÉTICAS

THE QUATERNARY CHALCOGENIDE COMPOUND $Ag_2FeGeSe_4$: A REVISION OF THEIR CRYSTAL STRUCTURE AND MAGNETIC PROPERTIES

EL COMPUESTO CALCOGENURO CUATERNARIO $Ag_2FeGeSe_4$: UNA REVISIÓN DE SU ESTRUCTURA CRISTALINA Y PROPIEDADES MAGNÉTICAS

DELGADO, Gerzon E.[1*]; DELGADO-NIÑO, Pilar[2], QUINTERO, Eugenio[3]

[1] Laboratorio de Cristalografía, Departamento de Química, Facultad de Ciencias, Universidad de Los Andes, Mérida, Venezuela

[2] Departamento de Ingeniería Ambiental, Facultad de Ingeniería, Universidad Libre, Bogotá, Colombia

[3] Centro de Estudios de Semiconductores, Departamento de Física, Facultad de Ciencias, Universidad de Los Andes, Mérida, Venezuela

** Correspondence author*
e-mail: gerzon@ula.ve

Received 8 April 2021; received in revised form 18 May 2021; accepted 22 June 2021

RESUMO

Introdução: Quaternary compounds bellowing to the I_2-II-IV-VI_4 system are of considerable technological interest due to their possible use in the preparation of solar cell and thermoelectric materials devices. In recent years considerable attention has been focused on the detailed study of quaternary chalcogenide compounds related to the chalcopyrite compounds, particularly $AgInSe_2$ which has emerged as a leading material for the preparation of photovoltaic devices due to their potential applications in solar cell technology. **Objetivos**: This work focuses on the synthesis, chemical analysis, thermal study, magnetism measurement and crystal structural characterization of the quaternary semiconductor $Ag_2FeGeSe_4$, an important member of the family I_2-II-IV-VI_4. **Métodos**: This material was synthesized by the melt and anneal technique, the chemical analysis was carried out by scanning electron microscopy (SEM), thermal study was performed by differential thermal analysis (DTA) measurements, magnetic susceptibility (χ) as a function of temperature and magnetization as a function of the magnetic field were performed, and crystal structure analysis was made employing the Rietveld method with powder X-ray diffraction data. **Resultados e Discussão**: The preparation confirms the formation of the quaternary compound with stoichiometric 2:1:1:4 according to the chemical analysis. This quaternary compound melt at 1015 K, and show an antiferromagnetic behavior with Neel temperature T_N of 240 K. The Debye temperature (θ_D) estimated for this compound was 194 K. The quaternary chalcogenide compound $Ag_2FeGeSe_4$ crystallizes in the orthorhombic space group $Pmn2_1$, Z = 4, with unit cell parameters: a = 7.6478(1) Å, b = 6.5071(1) Å, c = 6.4260(1) Å, and V = 319.79(1) Å^3, in a wurtzite-stannite arrangement with a Cu_2CdGeS_4-type structure, which is characterized by a three-dimensional arrangement of slightly distorted $AgSe_4$, $FeSe_4$, and $GeSe_4$ tetrahedra connected by corners. In this structure, each Se atom is coordinated by four cations located at the corners of a slightly distorted tetrahedron, and each cation is tetrahedrally bonded to four anions. **Conclusão**: The melt and anneal method remains effective for preparing compounds chalcogenides as the quaternary $Ag_2FeGeSe_4$, a new member of I_2-II-IV-VI_4 family of semiconductors which crystallizes in the non-centrosymmetric space group $Pmn2_1$ with diamond-like structure. The crystal structure information of this compound allows explaining their magnetic properties which in combination with its semiconductor properties make this material a potential aspirant for different applications, mainly in solar cells.

Palavras-chave: *Semicondutores, difração de raios-X em pó, estrutura cristalina, método de Rietveld, magnetismo.*

ABSTRACT

Background: Quaternary compounds bellowing to the I_2-II-IV-VI_4 system are of considerable technological interest due to their possible use in the preparation of solar cell and thermoelectric materials devices. In recent years, considerable attention has been focused on the detailed study of quaternary chalcogenide compounds related to the chalcopyrite compounds, particularly $AgInSe_2$, which has emerged as a leading material for the

DOI: 10.52571/PTQ.v18.n38.2021.07_DELGADO_pgs_85_99.pdf

preparation of photovoltaic devices due to their potential applications in solar cell technology. **Aims**: This work focuses on synthesis, chemical analysis, thermal study, magnetism measurement, and crystal structural characterization of the quaternary semiconductor $Ag_2FeGeSe_4$, an essential member of the family I_2-II-IV-VI_4. **Methods**: This material was synthesized by the melt and anneal technique. The chemical analysis was carried out by scanning electron microscopy (SEM) and differential thermal analysis (DTA). Magnetic susceptibility (χ) as a function of temperature and magnetization as a function of the magnetic field were also performed, and crystal structure analysis was made employing the Rietveld method with powder X-ray diffraction data. **Results and Discussion**: The preparation confirms the formation of the quaternary compound with stoichiometric 2:1:1:4 according to the chemical analysis. This quaternary compound melt at 1015 K, and show an antiferromagnetic behavior with Neel temperature T_N of 240 K. The Debye temperature (θ_D) estimated for this compound was 194 K. The quaternary chalcogenide compound $Ag_2FeGeSe_4$ crystallizes in the orthorhombic space group *Pmn2₁*, Z = 4, with unit cell parameters: *a* = 7.6478(1) Å, *b* = 6.5071(1) Å, *c* = 6.4260(1) Å, and V = 319.79(1) Å^3, in a wurtzite-stannite arrangement with a Cu_2CdGeS_4-type structure, which is characterized by a three-dimensional arrangement of slightly distorted $AgSe_4$, $FeSe_4$, and $GeSe_4$ tetrahedra connected by corners. In this structure, each Se atom is coordinated by four cations located at the corners of a slightly distorted tetrahedron, and each cation is tetrahedrally bonded to four anions. **Conclusions**: The melt and anneal method remains effective for preparing compounds chalcogenides as the quaternary $Ag_2FeGeSe_4$, a new member of I_2-II-IV-VI_4 family of semiconductors, which crystallizes in the non-centrosymmetric space group *Pmn2₁* with diamond-like structure. The crystal structure information of this compound allows explaining their magnetic properties, which in combination with its semiconductor properties make this material a potential aspirant for different applications, mainly in solar cells.

Keywords: *Semiconductors, powder X-ray diffraction, crystal structure, Rietveld method, Magnetism.*

RESUMEN

Antecedentes: Los compuestos cuaternarios pertenecientes al sistema I_2-II-IV-VI_4 son considerados de interés tecnológico debido a sus posibles usos en la preparación de celdas solares y dispositivos como materiales termoeléctricos. En años recientes, una considerable atención se ha enfocado en el estudio detallado de compuestos calcogenuros cuaternarios, particularmente AgInSe2, el cual ha emergido como un material líder en la preparación de dispositivos fotovoltaicos debido a sus potenciales usos en tecnología de celdas solares. **Objetivos**: Este trabajo se enfoca en la síntesis, análisis químico, estudio térmico, medidas de magnetismo y la caracterización estructural del semiconductor cuaternario $Ag_2FeGeSe_4$, un importante miembro de la familia I_2-II-IV-VI_4. **Métodos**: Este material se sintetizó utilizando la técnica de fusión y recocido. El análisis químico se llevó a cabo por microscopia electrónica de barrido (SEM) y por análisis térmico diferencial (DTA). Se realizaron medidas de susceptibilidad magnética (χ) como función de la temperatura y de la magnetización (M) como función del campo aplicado, y el análisis de la estructura cristalina se realizó empleando el método de Rietveld con datos de difracción de rayos-X en muestras policristalinas. **Resultados y discusiones**: La preparación confirmó la formación del compuesto cuaternario con estequiometria 2:1:1:4 de acuerdo con el análisis químico. Este compuesto cuaternario funde a1015 K, y muestra un comportamiento anti ferromagnético con una temperatura de Neel T_N de 240 K. La temperatura de Debye (θ_D) estimada para este compuesto es de 194 K.El compuesto calcogenuro cuaternario $Ag_2FeGeSe_4$ cristaliza en el grupo especial ortorrómbico *Pmn2₁*, Z = 4, con parámetros de celda unidad : *a* = 7.6478(1) Å, *b* = 6.5071(1) Å, *c* = 6.4260(1) Å, y V = 319.79(1) Å^3, en un arreglo wurtzita-estanita con estructura tipo Cu_2CdGeS_4, la cual se caracteriza por un arreglo tridimensional de tetraedros $AgSe_4$, $FeSe_4$, y $GeSe_4$ ligeramente distorsionados conectados por las esquinas. En esta estructura, cada átomo de selenio esta coordinado a cuatro cationes localizados en las esquinas de un tetraedro ligeramente distorsionado, y cada catión, a su vez, esta enlazado tetraédricamente a cuatro aniones. **Conclusions**: El método de fusión y recocido sigue siendo efectivo en la preparación en compuestos calcogenuros como el cuaternario $Ag_2FeGeSe_4$, un nuevo miembro dela familia de semiconductores I_2-II-IV-VI_4, los cuales cristalizan in el grupo espacial no-centrosimétrico con una estructura tipo diamante. La información sobre la estructura cristalina de este compuesto permite explicar sus propiedades magnéticas las cuales en combinación con sus propiedades semiconductoras hacen de este material un potencial aspirante para diferentes aplicaciones, principalmente in celdas solares.

Palabras clave: *Semiconductores, difracción de rayos-X en muestras policristalinas, estructura cristalina, método de Rietveld, magnetismo.*

1. INTRODUCTION:

The family of quaternary diamond-like semiconductors: I_2-II-IV-VI_4 with (I = Cu, Ag; II = Zn, Cd, Mn, Fe; IV = Ge, Sn; VI = S, Se) are formed from the tetrahedrally coordinated derivatives of the II-VI binaries (Parthé, 1995; Nikiforov, 1999) and can be defined as tetrahedral chalcogenides because their closest neighbors fourfold surround anions and cations. These materials have received increasing consideration for their promising physical properties and wide applications, mainly the Cu-based compounds which have been used as thermoelectric materials (Shi *et al*., 2009; Sevik and Cagin, 2010; Ibañez *et al*., 2012), solar-cell (Guo *et al*., 2009; Ahn *et al*., 2010; Todorov *et al*., 2010) and photocatalysts (Tsuji *et al*., 2010). Cu_2ZnSnS_4, for example, can be employed as photovoltaic devices because of its environmentally friendly thin-film solar-cell absorber, large absorption coefficient (~10^5 cm^{-1}), and optimum direct bandgap energy (~1.5 eV) (Wei *et al*., 2012; Liu *et al*., 2013).

When this family of semiconductor compounds is introduced, a paramagnetic cation as cation II, such as Mn^{+2}, Fe^{+2}, Co^{+2}, or Ni^{+2}, higher capacity as magneto-optical materials are produced (Shapira *et al*., 1988). These types of materials are known as semimagnetic compounds.

This family of quaternary compounds complies with the rules of adamantane formation (Parthé, 1995). According to this rule, when substituting cations, the average number of valence electrons per atom (4) and the ratio of valence electrons to the number of anions (8) are maintained. The general composition diagram for these quaternary compounds and their related binary and ternary compounds can be represented as shown in Figure 1.

From the structural point of view, these materials crystallize in sphalerite derivatives with tetragonal symmetry in a Cu_2FeSnS_4-type structure (stannite, space group $I\bar{4}2m$) or a Cu_2ZnSnS_4-type structure (kesterite, space group $I\bar{4}$) (Hall *et al*., 1978), or wurtzite derivatives with orthorhombic symmetry in a Cu_2CdGeS_4-type structure (wurtzite-stannite, space group $Pmn2_1$) (Parthé *et al*., 1969) or with monoclinic symmetry (wurtzite-kesterite, space group *Pn*) (Joubert-Bettan *et al*., 1969). Figure 2 shows the unit cells of each of the structures mentioned above. The slight differences lie in the distribution of the cations in the tetrahedral sites. It has been shown that there is a close relationship between the properties of the wurtzite-kesterite and kesterite structures as between wurtzite-stanite and stannite structures (Chen *et al*., 2010).

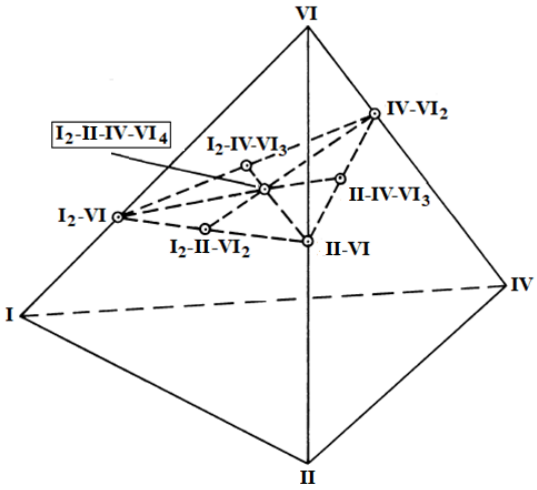

Figure 1. *General composition diagram showing the I_2-II-IV-VI_4 compounds.*

Several studies carried out in recent years on the structural characterization and physical properties of these I_2-II-IV-VI_4 quaternary semiconductor chalcogenides have been reported (Delgado *et al*., 2004; Quintero *et al*., 2007; Caldera *et al*., 2008; Moreno *et al*., 2009; Rincón *et al*., 2011; Dong *et al*., 2015; Wei and Nolas, 2015; Delgado *et al*., 2018). Nevertheless, the semimagnetic compounds of the Ag_2-II-IV-VI_4 family have received minor attention, although these Ag-based quaternary compounds also exhibit remarkable magnetic properties (Parasuk *et al*., 2002; Parasyuk *et al*., 2005; Davydyuk *et al*., 2011; Brunetta *et al*., 2012a; Brunetta *et al*., 2012b; Quintero *et al*., 2001; Wooley *et al*., 2003; Marquina *et al*., 2017), with photocatalyst and photo-electrochemical applications as in the case of Ag_2ZnSnS_4 (Li *et al*., 2013; Yeh and Cheng, 2014).

Table 1 shows the structural information found in the literature about the Ag_2-II-IV-VI_4 quaternary compounds with II= Mn, Fe, Zn, Cd, IV= Si, Ge, Sn, and VI= S, Se, Te, where the more relevant crystallographic parameters as unit cell, volume and bond distances together with the crystalline system and the space group are shown. Is possible observe that most compounds with detailed structural studies are those containing sulfur as anion.

In particular, as regards the quaternary $Ag_2FeGeSe_4$, which could be of interest because it was reported that it shows antiferromagnetic behavior down to 60K and an appreciably larger ferromagnetic effect below this temperature

(Wooley *et al*., 2003), and a low-temperature phase was identified in the equilibrium phase space of the system Ag-Fe-Ge-Se using thermodynamic calculations (Moroz *et al*., 2021). However, its crystal structure has not been established.

In the literature and crystallographic databases, Powder Diffraction File (PDF-ICDD, 2019), Inorganic Crystal Structure Database (ICSD, 2018), and Springer Materials (SpringerMaterials, 2021) only appear to report the same information corresponding only with the cell parameters obtained from a Güinier X-ray photographic data study (Quintero *et al*., 1999), without structural details such as the space group and atomic positions of cations and anions in the crystal packing.

The structural characterization of this quaternary compound could be used to explain and understand its interesting magnetic properties reported, and for this reason, this work is focused on the synthesis and complete crystal structure analysis of the semimagnetic compound $Ag_2FeGeSe_4$ using powder X-ray diffraction data.

2. MATERIALS AND METHODS:

2.1. Synthesis

The sample was synthesized by the melt and annealed technique. Highly pure components (silver 99.98 %, iron 99.97 %, germanium 99.99 %, and selenium 99.99 from Goodfellow) of 1 g sample were sealed under vacuum (≈ 10^{-5} Torr) in a small quartz ampoule which had previously been carbonized to prevent interaction of the components with the quartz. The components were heated up to 470 K and kept for about 1-2 h, and then the temperature was raised to 770 K using a rate of 40 K/h and held at this temperature for 14 hours. After, the sample was heated from 770 °C to 1070 K at a rate of 30 K/h and kept at this temperature for another 14 hours. Then it was raised to 1420 K at 60 K/h, and the components were melted together at this temperature. The furnace temperature was brought slowly (4 K/h) down to 870 K, and the sample was annealed at this temperature for 1 month. Then, the sample was slowly cooled to room temperature using a rate of about 2 K/h.

2.2. Chemical analysis (EDS)

The stoichiometric relations of the sample were investigated by scanning electron microscopy (SEM) technique, using Hitachi S2500 equipment. The microchemical composition was found by an energy-dispersive X-ray spectrometer (EDS) coupled with a computer-based multichannel analyzer (MCA, Delta III analysis, and Quantex software, Kevex). For the EDS analysis, K_α lines were used. The accelerating voltage was 15 kV. The samples were tilted 35 degrees. A standardless EDS analysis was made with a relative error of ± 5-10% and detection limits of the order of 0.3 wt %, where the k-ratios are based on theoretical standards. Table 2 shows the experimental results on the stoichiometry of the quaternary $Ag_2FeGeSe_4$, for which three different regions of the ingot were evaluated. These results indicate that the composition corresponds to the ratio 2: 1: 1:4.

2.3. Thermal analysis (DTA)

Differential thermal analysis (DTA) measurements were obtained, in the temperature range between 295 and 1150 K, using a Perkin-Elmer DTA-7 with aluminum and gold used as reference materials. The charge was of a powdered sample of approximately 100 mg weight. The error in determining these temperatures is about ±10K. The value of the melting point for the compound was obtained from the peaks on the DTA cooling curve. Melting temperature was determined from the baseline intercept of the tangent to the leading edge of the peak in the difference signal. The cooling DTA melting peak is shown in Figure 3. $Ag_2FeGeSe_4$ melt at 1015 K.

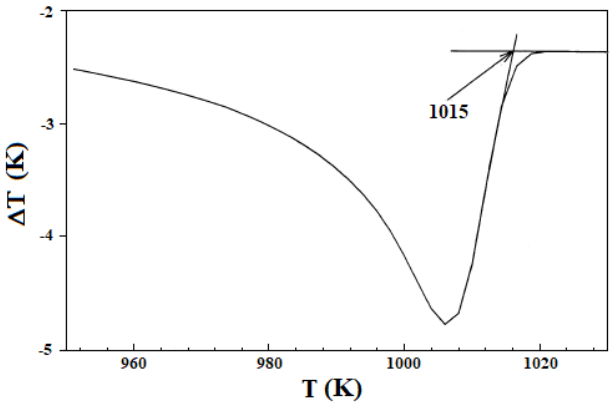

***Figure 3**. DTA curve for the quaternary $Ag_2FeGeSe_4$.*

2.4. Magnetization measurement

Measurements of magnetic susceptibility (χ) as a function of temperature (T) were made using a Quantum Design SQUID magnetometer with an external magnetic field of $1x10^{-2}$ T. Measurements were made in the range of 2 to 300

K. The magnitude of χ vs T variations serves to determine the temperatures at which magnetic transitions occurred and to estimate the type of transition.

Figure 4 shows the magnetic susceptibility curves (χ vs T) in the temperature range 2K to 300 K., where are shown the heating curve (zero-field cooled) and cooling curve (field cooled). The form of the curves indicates that the transition is an antiferromagnetic type, with Neel temperature T_N of 240 K, and a weak ferromagnetic contribution, which has been observed previously in similar compounds (Quintero *et al*., 2001).

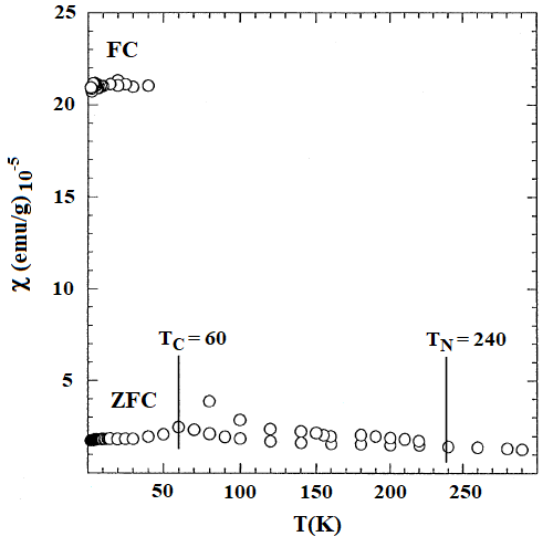

Figure 4*. Variation of magnetic susceptibility (χ) with temperature (T) for zero-field cooled (ZFC) and field cooled (FC) conditions. Vertical lines show transitions T_N and T_C.*

Measurements of magnetization (M) as a function of applied field (B) were made at helium temperatures using the high field pulsed technique for fields up to 35 T, and using the SQUID steady-field system with fields up to 6 T. Figure 5 show the variations of M with B for the quaternary $Ag_2FeGeSe_4$. In this figure is possible observe the spin-flop behavior for measurements using pulsed field system, where an appreciable hysteresis is present with a B_f with a value of approximately 16 T.

These results indicate that $Ag_2FeGeSe_4$ has a Neel temperature of 240 K and shows mainly antiferromagnetic behavior with a very weak superimposed ferromagnetic component down to 60K. At 4.2 K, a transition occurs resulting in an appreciably larger ferromagnetic effect below the transition.

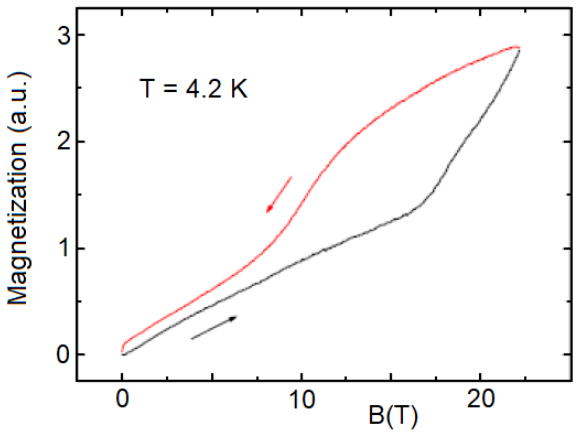

Figure 5. *Magnetization measurement (M) vs applied magnetic field (B) of the chalcogenide $Ag_2FeGeSe_4$ at 4.2 K.*

Additionally, the Debye temperature θ_D, was calculated by using the Lindemann's expression $\theta_D \approx C\,(T_M/W)^{1/2}(1/a_e)$ (Deus *et al*., 1981). Where, *C* is a constant (*C* ≈ 300 for I_2-II-IV-VI_4 tetrahedral bonded quaternary compounds) (Dong *et al*., 2015), T_M is the melting temperature of the compound (1015 K), *W* is the molecular weight, and a_e is the effective lattice parameter $a_e = (V/Z)^{1/3}$ (a_e = 5.7354 Å) where *V* is the volume of the unit cell (in Å^3) and *Z* the number of molecules per cell (Z = 2). For $Ag_2FeGeSe_4$ the θ_D value obtained was ≈ 194 K, which agree well with those reported, from 185 to 310 K (Quintero *et al*., 2014),.for related semimagnetic semiconductor compounds.

2.5. Powder X-ray diffraction (PXRD)

A small quantity of the sample was ground in an agate mortar and pestle. The resulting fine powder, sieved to a grain size of fewer than 46 μm, was mounted on a flat zero-background holder. The X-ray diffraction data were measured, in θ/θ reflection mode, using a Siemens D5005 diffractometer equipped with an X-ray tube (CuKα radiation: λ = 1.5418 Å; 40kV, 30 mA) and a diffracted beam graphite monochromator. Data were collected at room temperature. The specimen was scanned in the 2θ range of 10 to 80°, the scan step was 0.02°, and the time of counting in every step was 10 s. Quartz was used as an external standard. The precise determination of peak positions was carried out employing the Winplotr analytical software (Roisnel and Rodríguez-Carvajal, 2001).

3. RESULTS AND DISCUSSION:

Figure 6 shows the resulting powder X-ray diffraction pattern for the $Ag_2FeGeSe_4$ compound. A single-phase is observed. The powder pattern was indexed using the Dicvol program (Boultif and Löuer, 2004). An orthorhombic cell of dimensions *a* = 7.650(1) Å, *b* = 6.508(1) Å, and *c* = 6.425(1) Å was obtained. These cell values are close to those previously reported in PDF: 052-0986 (PDF-ICDD, 2019). The systematic absence indicated a *P*-type cell. The crystallographic characteristics of $Ag_2FeGeSe_4$, such as the sample composition, cell parameters, and lattice-type indicate that this material crystallizes with a Cu_2CdGeS_4-type structure (Parthé et al., 1969) similarly with other related I_2-II-IV-VI_4 compounds. So, to refine the structural parameters of $Ag_2FeGeSe_4$, the space group *Pmn2₁* (Nº 31) and the atomic position parameters of Cu_2CdGeS_4 were taken as the starting values.

The Rietveld refinement (Rietveld, 1969) was performed using the Fullprof program (Rodríguez-Carvajal, 1993; Rodríguez-Carvajal, 2021). The refinement parameters were scale factor, background, unit cell parameters, peak profile, atomic coordinates, and overall isotropic temperature factor. The unit cell parameters obtained in the indexing were used as starting data. The angular dependence was described using the Cagliotti formula (Cagliotti *et al*., 1958) and the peak shapes were described by the Thompson-Cox-Hastings pseudo-Voigt profile function (Thompson *et al*., 1987). The background was refined with a polynomial of six coefficients. An overall isotropic temperature factor was refined for described the thermal motion of the atoms. The final Rietveld refinement led to agreement factors of: R_p = 7.7%, R_{wp} = 8.4%, R_{exp} = 6.6%, and S = 1.3, for 4001 step intensities and 145 independent reflections. Table 3 summarizes the Rietveld refinement results. Figure 6 shows the observed calculated and different profile for the final cycle of the refinement. Atomic coordinates, occupancy factors, and isotropic temperature factors are given in Table 4. Figure 7 shows the unit cell diagram for $Ag_2FeGeSe_4$. Bond distances and angles are given in Table 5.

$Ag_2FeGeSe_4$ crystallize with orthorhombic symmetry, space group *Pmn2₁*, and unit cell parameters: *a* = 7.6478(1) Å, *b* = 6.5071(1) Å, *c* = 6.4260(1) Å, and V = 319.79(1) $Å^3$, in a wurtzite-stannite structure. This structure can be defined as closest-packed array, in hexagonal fashion, of selenide anions with Ag^+, Fe^{2+}, and Ge^{4+} occupying tetrahedral holes, and is characterized by a three-dimensional arrangement of slightly distorted $AgSe_4$, $FeSe_4$, and $GeSe_4$ tetrahedra connected by corners. Every Ag, Fe, or Ge atom is surrounded by four Se atoms, forming $AgSe_4$, $FeSe_4$, or $GeSe_4$ units; every selenium atom has four nearest-neighbor atoms: two Ag atoms, one Fe atom, and one Ge atom. This array is expected for adamantane compounds (Parthé, 1995).

The tetrahedrons containing the Ge atoms [mean Se…Se distance 3.470(9) Å] are slightly smaller than those containing the Fe atoms [means Se…Se distance 3.946(9) Å] and Ag atoms [mean Se…Se distance 3.996(9) Å] respectively. The bond distances are slightly shorter than the sum of the ionic radii of the atoms involved (rAg^+ = 1.14 Å, rFe^{2+} = 0.77 Å, rGe^{4+} = 0.53 Å, rSe^{2-} = 1.84 Å) for structures tetrahedrally bonded (Shannon, 1976). Bond distances in Table 5 show an average Ag-Se bond length of 2.450(8) Å. This distance compare well to those found for the related ternary $AgInSe_2$ with 2.612(2) Å (Delgado *et al*., 2015) and for the quaternary $Ag_2CdSnSe_4$ with 2.572(2) Å (Parasyuk *et al*., 2002). The Fe-Se bond has an average length of 2.417(8) Å which compare well with those observed in compounds as CuFe(Al,Ga,In)Se_3 (Mora *et al*., 2007) and $CuFe_2$(Al,Ga,In)Se_4 (Delgado *et al*., 2008). The Ge-Se [mean value 2.126(8) Å] is also in good agreement with similar distances in Cu_2GeSe_3 (Rincón *et al*., 2008), Cu_2GeSe_4 (Chi *et al*., 2013; Delgado *et al*., 2015) $Cu_2ZnGeSe_4$ (Parayuk *et al*., 2001) and $Cu_2CdGeSe_4$ (Gulay *et al*., 2002). All these structures were found in the Inorganic Crystal Structure Database (ICSD, 2018).

4. CONCLUSIONS:

The quaternary chalcogenide compound $Ag_2FeGeSe_4$ was synthesized by the melt and anneals technique from the pure elements and its crystal structure was characterized by X-ray diffraction analysis. Rietveld refinement from the powder X-ray data allowed us to determine the crystal structure of this compound.

This compound crystallizes in the wurtzite-stannite structure, space group *Pmn2₁*, characterized by a three-dimensional arrangement of slightly distorted $AgSe_4$, $FeSe_4$, and $GeSe_4$ tetrahedra connected by corners, and correspond to one new member of the quaternary chalcogenide material belonging to the I_2-II-IV-VI_4 family of semiconductors.

This quaternary compound melt at 1015 K, and show an antiferromagnetic behavior with Neel temperature T_N of 240 K. The Debye temperature

(θ_D) estimated for this compound was 194 K.

The crystal structure information of this compound allows explaining their magnetic properties which in combination with its semiconductor properties make this material a potential aspirant for different applications, mainly in solar cells.

5. ACKNOWLEDGMENTS:

The authors want to thank CDCHT-ULA and FONACIT, Venezuela.

6. REFERENCES:

1. Ahn, S., Jung, S., Gwak, J., Cho, A., Shin, K., Yoon, K., Park, D., Cheong, H., Yun, J.H. (2010). Determination of band gap energy of thin films: On the discrepancies of reported band gap values. *Applied Physics Letters, 97*(2): 0219051-3. https://doi.org/10.1063/1.3457172.
2. Boultif, A., Löuer, D. (2004). Powder pattern indexing with the dichotomy method. *Journal of Applied Crystallography, 37*(5)**:** 724-731. http://dx.doi.org/10.1107/S0021889804014876.
3. Brunetta, C.D., Balamurugan, K., Rosmus, K.A., Aitken, J.A. (2012a). The crystal and electronic band structure of the diamond-like semiconductor Ag_2ZnSiS_4. *Journal of Alloys and Compounds, 516*(1-2): 65-72. https://doi.org/10.1016/j.jallcom.2011.11.133.
4. Brunetta, C.D., Brant, J.A., Rosmus, K.A., Henline, K.M., Karey, E., MacNeil, J.H., Aitken, J.A. (2013). The impact of three new quaternary sulfides on the current predictive tools for structure and composition of diamond-like materials. *Journal of Alloys and Compounds, 574*(8): 495-503. http://dx.doi.org/10.1016/j.jallcom.2013.05.141.
5. Brunetta, C.D., Minsterman III, W.C., Lake, C.H., Aitken, J.A. (2012b). Cation ordering and physicochemical characterization of the quaternary diamond-like semiconductor Ag_2CdGeS_4. *Journal of Solid State Chemistry, 187*(3): 177-185. http://dx.doi.org/10.1016/j.jssc.2011.12.032.
6. Cagliotti, G., Paoletti, A., Ricci, F.P. (1958). Choice of collimators for a crystal spectrometer for neutron diffraction. *Nuclear Instruments, 3*(4): 223-228. http://dx.doi.org/10.1016/0369-643X(58)90029-X.
7. Caldera, D., Quintero, M., Morocoima, M., Quintero, E., Grima, P., Marchan, M., Moreno, E., Bocaranda, P., Delgado, G.E., Mora, A.E., Briceño, J.M., Fernandez, J.L. (2008). Lattice parameters values and phase diagram for the $Cu_2Zn_{1-z}FezGeSe_4$ alloy system. *Journal of Alloys and Compounds, 457*(1-2): 221-224. https://doi.org/10.1016/j.jallcom.2007.03.033.
8. Caye, R., Laurent, Y., Picot, P., Pierrot, R., Levy, C. (1968). La hocartite, Ag_2SnFeS_4, une nouvelle espece minerale. *Bulletin de la Societe Francaise de Mineralogie et de Cristallographie, 91*(4): 383-387. https://www.persee.fr/doc/bulmi_0037-9328_1968_num_91_4_6244.
9. Chen, W., Waslsh, A., Luoe, Y., Yang, J.H., Gong, X.G., Wei, S.H. (2010). Wurtzite-derived polytypes of kesterite and stannite quaternary chalcogenide semiconductors. *Physical Review B: covering condensed matter and materials physics, 82*(19): 195203. https://doi.org/10.1103/PhysRevB.82.195203.
10. Choi, S.G., Donohue, A.L., Marcano, G., Rincón, C., Gedvilas, L.M., Li, J., Delgado, G.E. (2013). Optical properties of cubic-phase Cu_2GeSe_4 single crystal. *Journal of Applied Physcis, 114*(3): 033531. https://doi.org/10.1063/1.4816051.
11. Davydyuk, G.E., Myronchuka, G.L., Kittyk, I.V., Danyl'chuk, S.P., Bozhko, V.V., Parasyuk, O.V. (2011). Ag_2CdSnS_4 single crystals as promising materials for optoelectronic. *Optical Materials, 33*(8): 1302-1306. https://doi.org/10.1016/j.optmat.2011.03.003.
12. Delgado, G.E., Contreras, J.E., Marcano, G., Rincón, C., Nieves, L. (2015). Caracterización estructural del semiconductor ternario Cu_2GeSe_4. *Revista LatinoAmericana de Metalurgia y Materiales, 35*(1): 34-38. http://www.rlmmjournal.com/index.php/path/article/download/120/118.

13. Delgado, G.E., Mora, A.J., Grima-Gallardo, P., Quintero, M. (2008). Crystal structure of $CuFe_2InSe_4$ from X-ray powder diffraction. *Journal of Alloys and Compounds, 454*(1-2): 306-309. https://doi.org/10.1016/j.jallcom.2006.12.057.

14. Delgado, G.E., Mora, A.J., Pineda, C., Ávila, R., Paredes, S. (2015). X-ray powder diffraction data and Rietveld refinement of the ternary semiconductor chalcogenides $AgInSe_2$ and $AgInTe_2$. *LatinAmerican Journal of Metallurgy and Materials, 35*(1): 110-117. http://www.rlmm.org/ojs/index.php/rlmm/article/view/546.

15. Delgado, G.E., Quintero, E., Tovar, R., Quintero, M. (2004). X-ray powder diffraction study of the semiconducting alloy $Cu_2Cd_{0.5}Mn_{0.5}GeSe_4$. *Crystal Research and Technology, 39*(9): 807-810. https://doi.org/10.1002/crat.200310257.

16. Delgado, G.E., Sierralta, N., Quintero, E., Quintero, M., Quintero, E., Moreno, E., Flores, J.A., Rincón, C. (2018). Synthesis, structural characterization and differential thermal analysis of the quaternary compound Ag_2MnSnS_4. *Revista Mexicana de Física, 64*(3): 216-221. https://doi.org/10.31349/RevMexFis.64.216.

17. Deus, P., Schneider, H.A., Voland, U. (1981). Estimation of the Debye temperature of diamond-like semiconducting compounds by means of the Lindemann rule. *Crystal Research and Technology, 16*(8): 941-948. https://doi.org/10.1002/crat.19810160814.

18. Dong, Y., Wojtas, L., Martin, J., Nolas, G.S. (2015). Synthesis, crystal structure, and transport properties of quaternary tetrahedral chalcogenides. *Journal of Materials Chemistry C, 3*(40): 10436-10441. https://doi.org/10.1039/C5TC01606A.

19. Friedrich, D., Greil, S., Block, T., Heletta, L., Pöttgen, R., Pfitzner, A. (2018). Synthesis and characterization of Ag_2MnSnS_4, a new diamond-like semiconductor. *Zeitschrift für anorganische und allgemeine Chemie, 644*(24): 1707-1714. http://dx.doi.org/10.1002/zaac.201800142.

20. Gulay, Y.E., Romanyuk, L.V., Parasyuk, L.D. (2002). Crystal structures of low- and high-temperature modifications of $Cu_2CdGeSe_4$. *Journal of Alloys and Compounds, 347*(1-2): 193-197. https://doi.org/10.1016/S0925-8388(02)00790-9.

21. Guo, Q., Hillhouse, W.W., Agrawal R. (2009). Synthesis of Cu_2ZnSnS_4 nanocrystal ink and its use for solar cells. *Journal of American Chemical Society, 131*(33): 11672-11673. https://doi.org/10.1021/ja904981r.

22. Hall, S.R., Szymanski, J.T., Stewart, J.M. (1978). Kesterite, $Cu_2)(Zn,Fe)SnS_4)$, and stannite, $Cu_2)(Fe,Zn)SnS_4)$, structurally similar but distinct minerals. *Canadican Mineralogist, 16*(2): 131-137. http://canmin.geoscienceworld.org/content/16/2/131.extract.

23. Ibañez, M., Cacavid, M., Zamani, R., García-Castelló, N., Izquierdo-Roca, V., Li, W., Fairbrother, A., Prades, J.D., Shavel, A., Arbiol, J., Pérez-Rodríguez, A., Morante, J.R., Cabot, A. (2012). Composition control and thermoelectric properties of quaternary chalcogenide nanocrystals: The case of stannite $Cu_2CdSnSe_4$. *Chemistry of Materials, 24*(3): 562-570. https://doi.org/10.1021/cm2031812.

24. ICSD-*Inorganic Crystal Structure Database*. Gemlin Institute, Kalrsruhe, Germany, 2018.

25. International Centre for Diffraction Data. *PDF-ICDD-Powder Diffraction File (Set 1-71)*. Newtown Square, PA, USA, 2019.

26. Johan, Z., Picot, P. (1982). La pirquitasite, Ag_2ZnSnS_4, un nouveau membre du groupe de la stannite. *Bulletin de la Societe Francaise de Mineralogie et de Cristallographie, 105*(3): 229-235. https://www.persee.fr/doc/bulmi_0180-9210_1982_num_105_3_7610.

27. Joubert-Bettan, C.A., Lachenal, R., Bertaut, E.F., Parthé, E. (1969). The crystal structures of Na_2ZnSiO_4, Na_2ZnGeO_4, and Na_2MgGeO_4. *Journal of Solid State Chemistry, 1*(1): 1-5. https://doi.org/10.1016/0022-4596(69)90001-2.

28. Li, K., Chai, B., Peng, T., Mao, J., Zan, L. (2013). Synthesis of multicomponent sulfide Ag_2ZnSnS_4 as an efficient

photocatalyst for H_2 production under visible light irradiation. *RSC Advances, 3*(1): 253-258. https://doi.org/10.1039/C2RA21481D.

29. Liu, W., Guo, B., Mak, C., Li., A., Wu, X., Zhang, F. (2013). Facile synthesis of ultrafine Cu_2ZnSnS_4 nanocrystals by hydrothermal method for use in solar cells. *Thin Solid Films, 535*(5): 39-43. https://doi.org/10.1016/j.tsf.2012.11.073

30. Marquina, J., Sierralta, N., Quintero, M., Rincón, C., Morocoima, M., Quintero, E. (2017). Study of the critical-fields and the thermal broadening in polycrystalline $Ag_2FeGeSe_4$ semiconducting compound. *Revista Mexicana de Física, 63*(5): 456-460. https://rmf.smf.mx/ojs/rmf/article/view/366/211.

31. Mora, A.J., Delgado, G.E., Grima-Gallardo, P. (2007). Crystal structure of $CuFeInSe_3$ from X-ray powder diffraction data. *physica status solidi (a): applications and materials science, 204* (2): 547-554. https://doi.org/10.1002/pssa.200622395.

32. Moreno, E., Quintero, M., Morocoima, M., Quintero, E., Grima-Gallardo, P., Tovar, R., Bocaranda, P., Delgado, G.E,, Contreras, J.E., Mora, A.E., Briceño, J.M., Avila, R., Fernandez, J.L., Henao, J.A., Macías, M.A. (2009). Lattice parameter values and phase transitions for the $Cu_2Cd_{1-z}Mn_zSnSe_4$ and $Cu_2Cd_{1-z}Fe_zSnSe_4$ alloys". *Journal of Alloys and Compounds, 486*(1-2): 212-218. https://doi.org/10.1016/j.jallcom.2009.07.066.

33. Moroz, M., Tesfaye, F., Demchenko, P., Prokhorenko, M., Rudyk, B., Soliak, L., Lindberg, D., Reshetnak, O., Hupa, L. (2021). Thermodynamic examination of quaternary compounds Ag-Fe-(Ge,Sn)-Se systems by solid-state EMF method. *In Materials Processing Fundamentals, The Minerals, metals & Materials Series*; JohnWiley & Sons, Ltd. Hoboken, NJ, USA, pp. 271-290. https://doi.org/10.1007/978-3-030-65253_1_24.

34. Nikiforov, K.G. Magnetically ordered multinary semiconductors. (1999). *Progress in Crystal Growth and Characterization of Materials, 39*(1-4): 1-104. https://doi.org/10.1016/S0960-8974(99)00016-9.

35. Parasyuk, L.D., Gulay, Y.E., Romanyuk, L.V., Piskach, L.V. (2001). Phase diagram of the Cu_2GeSe_3-ZnSe system and crystal structure of the $Cu_2ZnGeSe_4$ c compound. *Journal of Alloys and Compounds, 329*(1): 202-207. https://doi.org/10.1016/S0925-8388(01)01606-1.

36. Parasyuk, O.V., Fedorchuk, A.O., Kogut, Y.M., Piskach, L.V., Olekseyuk, I.D. (2010). The Ag_2S-ZnS-GeS_2 system: Phase diagram, glass-formation region and crystal structure of Ag_2ZnGeS_4. *Journal of Alloys and Compounds,* 500(1), 26-29. https://doi.org/10.1016/j.jallcom.2010.03.198.

37. Parasyuk, O.V., Gulay, L.D., Piskach, L.V., Olekseyuk, I.D. (2002). The Ag_2Se-CdSe-$SnSe_2$ system at 670 K and the crystal structure of the $Ag_2CdSnSe_4$ compound. *Journal of Alloys and Compounds, 335*(1-2): 176-180. https://doi.org/10.1016/S0925-8388(01)01845-X.

38. Parasyuk, O.V., Olekseyuk, I.D., Piskach, L.V., Volkov, S.V., Pekhnyo, V.I. (2015b). Phase relations in the Ag_2S-CdS-SnS_2 system and the crystal structure of the compounds. *Journal of Alloys and Compounds, 399*(1-2): 173-177. http://dx.doi.org/10.1016/j.jallcom.2005.03.023.

39. Parasyuk, O.V., Piskach, L.V., Olekseyuk, I.D., Pekhnyo, V.I. (2005a). The quasi-ternary system Ag_2S-CdS-GeS_2 and the crystal structure of Ag_2CdGeS_4. *Journal of Alloys and Compounds, 397*(1-2): 95-98. https://doi.org/10.1016/j.jallcom.2004.12.043.

40. Parthé, E., in: Westbrook JH, Fleischer RL (Eds.), *Intermetallic compounds, principles and applications*. Jhon Wiley & Sons; Chichester, UK, 1995. Vol 1, Chap. 14.

41. Parthé, E., Yvon, K., Deitch, R.H. (1969). The crystal structure of Cu_2CdGeS_4 and other quaternary normal tetrahedral structure compounds. *Acta Crystallographica Section B: Structural Science, Crystal Engineering and Materials, 25*(6): 1164-1174. http://dx.doi.org/10.1107/S0567740869003670.

42. Quintero, E., Tovar, R., Quintero, M., Delgado, G.E., Morocoima, M., Caldera, D., Ruiz. J., Mora, A.E., Briceño, J.M., Fernandez, J.L. (2007). Lattice parameter values and phase transitions for the $Cu_2Cd_{1-z}Mn_zGeSe_4$ and $Cu_2Cd_{1-z}Fe_zGeSe_4$ alloys. *Journal of Alloys and Compounds, 432*(1-2): 142-148. https://doi.org/10.1016/j.jallcom.2006.05.126.
43. Quintero, M., Barreto, A., Grima-Gallardo, P., Quintero, E., Sánchez Porras, G., Ruiz, J., Woolley, J.C., Lamarche, G., Lamarche, A.M. (1999). Crystallographic properties of I_2-Fe-IV-VI_4 magnetic semiconductor compounds. *Materials Research Bulletin, 34*(14-15): 2263-2270. https://doi.org/10.1016/S0025-5408(00)00166-5.
44. Quintero, M., Cadenas, R., Tovar, R., Quintero, E., Gonzalez, J., Ruiz, J., Woolley, J.C., Lamarche, J.C., Lamarche, A.M., Broto, J.M., Rakoto, H., Barbaste, R. (2001). Magnetic spin-flop and magnetic saturation in $Ag_2FeGeSe_4$, $Ag_2FeSiSe_4$ and $Cu_2MnGeSe_4$ semiconductor compounds. *Physica B: Consended Matter, 294-295*(1): 471-474. https://doi.org/10.1016/S0921-4526(00)00702-X.
45. Rietveld, H.M. (1969). A profile refinement method for nuclear and magnetic structures. *Journal of Applied Crystallography, 2*(2)**:** 65-71. https://doi.org/10.1107/S0021889869006558
46. Rincón, C., Marcano, G., Marín, G., Mora, A.J., Delgado, G.E., Herrera-Pérez, J.L., Mendoza-Alvarez, J.G., Rodríguez, P. (2008). Raman scattering and X-ray diffraction study in Cu_2GeSe_3. *Solid State Communications, 146*(1-2): 65-68. https://doi.org/10.1016/j.ssc.2008.01.018.
47. Rincón, C., Quintero, M., Moreno, E., Power, Ch., Quintero, E., Henao, J.A., Macías, M.A., Delgado, G.E., Tovar, R., Morocoima, M. (2011). X-ray diffraction, Raman spectrum and magnetic susceptibility of the magnetic semiconductor Cu_2FeSnS_4. *Solid State Communication, 151*(1-2): 947-951. https://doi.org/10.1016/j.ssc.2011.04.002.
48. Rodriguez-Carvajal J. (1993). Recent advances in magnetic structure determination by neutron powder diffraction. *Physica B: Condensed Matter, 192*(1-2)**:** 55-69. http://dx.doi.org/10.1016/0921-4526(93)90108-I.
49. Rodriguez-Carvajal, J. Fullprof program: Rietveld pattern matching analysis of powder patterns (version 7.4), Laboratoire Léon Brillouin (CEA-CNRS), France, 2021.
50. Roisnel, T., Rodríquez-Carvajal, J. (2001). WinPLOTR: A windows tool for powder diffraction pattern analysis. *Materials Science Forum, 378-381*(1): 118-123. https://www.scientific.net/MSF.378-381.118
51. Sevik, C., Cagin, T. (2010). *Ab initio* study of thermoelectric transport properties of pure and doped quaternary compounds. *Physical Review B: covering condensed matter and materials physics, 82*(4): 045202. http://dx.doi.org/10.1103/PhysRevB.82.045202.
52. Shannon, R.S. (1976). Revised effective ionic radii and systematic studies of interatomic distances in halides and chalcogenides. *Acta Crystallographica Section A: Foundations and Advances, 32*(5): 751-767. http://dx.doi.org/10.1107/S0567739476001551.
53. Shapira, Y., McNiff, E.J., Oliveira, N.F., Honig, E.D., Dwight, K., Wold, A. (1988). Magnetic properties of antiferromagnetic interactions in the wurtz-stannite structure. *Physical Review B: covering condensed matter and materials physics, 37*(1): 411-418. https://doi.org/10.1103/PhysRevB.37.411.
54. Shi, X.Y., Huang, F.Q., Liu, M.L., Chen, L.D. (2009). Thermoelectric properties of tetrahedrally bonded wide-gap stannite compounds $Cu_2ZnSn_{1-x}In_xSe_4$. *Applied Physics Letters, 94*(12): 122103. https://doi.org/10.1063/1.3103604.
55. SpringerMaterials, https://materials.springer.com. Access in 30/03/2021.
56. Thompson, P., Cox, D.E., Hastings, J.B. (1987). Rietveld refinement of Debye-Scherrer synchrotron X-ray data from Al_2O_3. *Journal of Applied Crystallography, 20*(): (1987) 79-83. http://dx.doi.org/10.1107/S0021889887087090.

57. Todorov, T.K., Reuter, K.B., Mitzi, D.B. (2010). High-efficiency solar cell with earth-abundant liquid-processed absorber. *Advanced Materials, 2*(22): E156-E159. https://doi.org/10.1002/adma.200904155.

58. Tsuji, I., Shimodaira, Y., Kato, H., Kobayashi, H., Kudo, A. (210). Novel stannite-type complex sulfide photocatalysts A^{I}_2-Zn-A^{IV}-S_4 (A^{I} = Cu and Ag; A^{IV} = Sn and Ge) for sydrogen evolution under visible-light irradiation. *Chemistry of Materials, 22*(4): 1402-1409. https://doi.org/10.1021/cm9022024.

59. Wei, K., Nolas, J.S. (2015). Synthesis, characterization and alloying of Cu_2ZnSnQ_4 (Q= S, Se and Te) nanocrystals. *Journal of Solid State Chemistry, 226*(3): 215-218. https://doi.org/10.1016/j.jssc.2015.02.027.

60. Wei, M., Du., Q., Wang, D., Liu, W., Jiang, G., Zhu, C. Synthesis of spindle-like kesterite $Cu_2Zn_SnS_4$ nanoparticles using thiorea as sulfur source. *Materials Letters, 79*(7): 177-179. https://doi.org/10.1016/j.matlet.2012.03.080

61. Wooley, J.C., Lamarche, G., Lamarche, A.M., Rakoto, H., Broto, J.M., Quintero, M., Morocoima, M., Quintero, E., Gonzalez, J., Tovar, R., Cadenas, R., Bocoranda, P., Ruiz, J. (2003). High field magnetic properties of $Ag_2FeGeSe_4$ in the temperature range 2-300 K. *Journal of Magnetism and Magnetic Materials, 257*(1): 87-94. https://doi.org/10.1016/S0304-8853(02)01051-X.

62. Yeh, L.-Y., Cheng, K.-W. (2014). Preparation of the Ag-Zn-Sn-S quaternary photoelectrodes using chemical bath deposition for photoelectrochemical applications. *Thin Solid Films, 558*(5): 289-293. https://doi.org/10.1016/j.tsf.2014.02.046.

7. OPEN ACCESS:

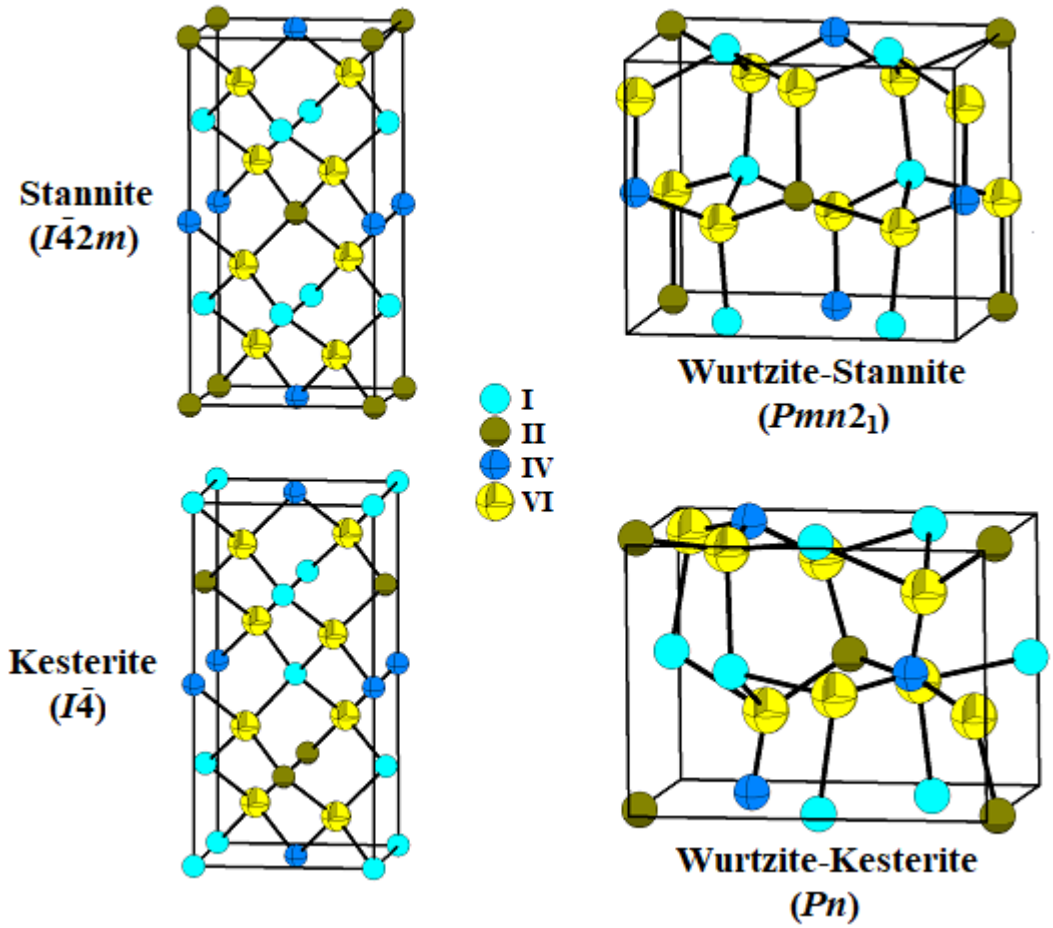

Figure 2. *Unit cell diagrams of the different structures that describe the I_2-II-IV-VI_4 family of compounds.*

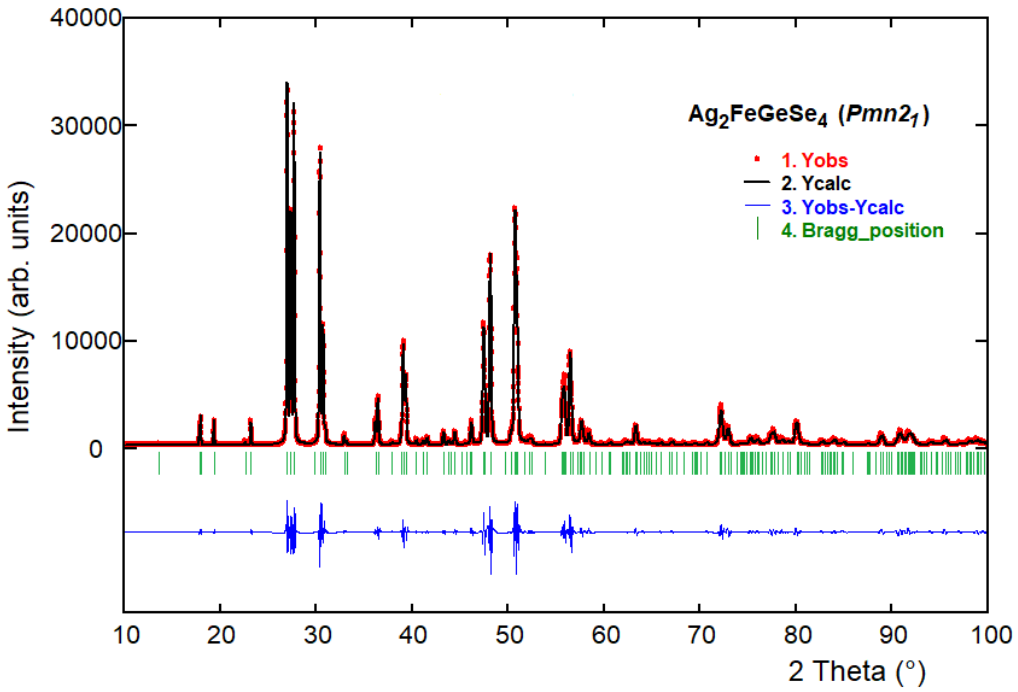

Figure 6. *Observed (·), calculated (-), and difference plot of the final Rietveld refinement of $Ag_2FeGeSe_4$. The Bragg reflections for the studied phase are indicated by vertical bars.*

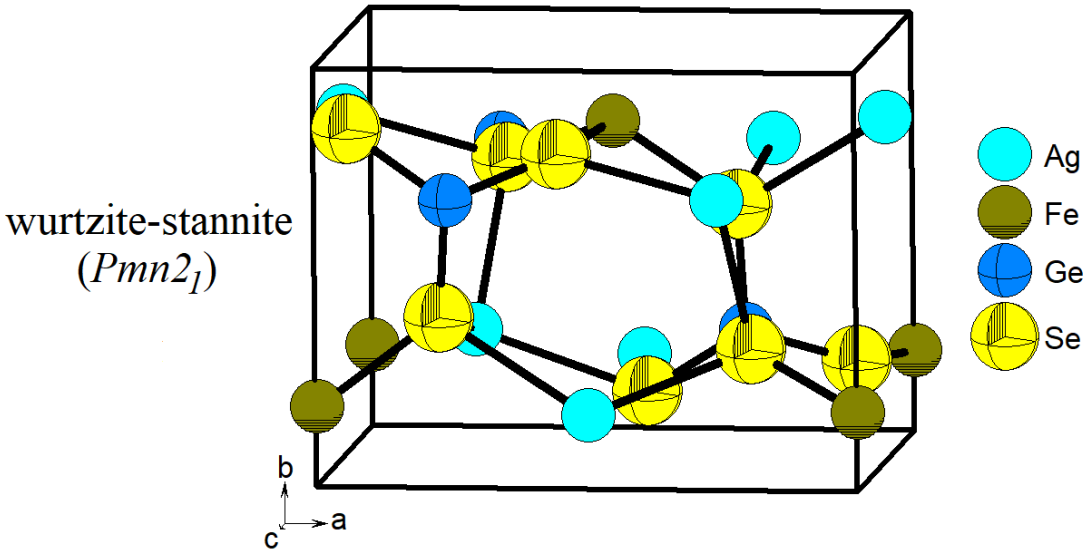

Figure 7. *Unit cell diagram of $Ag_2FeGeSe_4$ viewed in the* ***ba*** *plane of the space group $Pmn2_1$.*

***Table 1**. Crystallographic information about the quaternaries I_2-II-IV-VI_4 with I =Ag, II = Fe, Mn, Zn, Cd, IV = Si, Ge, Sn, VI = S, Se, Te.*

Molecular Formula	**System**	**Space group**	***a*, *b*, *c*, *β*** **(Å,°)**	**V (Å³)**	**Ag-VI (Å)**	**II-VI (Å)**	**IV-VI (Å)**	**Ref.**
Ag_2FeSiS_4	Mon.	*Pn* Z= 2	6.4220(1) 6.6185(1) 7.8650(1) 90.614(1)	334.28(1)	2.546(1)	2.354(1)	2.129(2)	Brunetta *et al*., 2013
Ag2FeSnS4	Tetr.	$I\bar{4}2m$ Z= 2	5.74(3) 10.96(5)	361.11	-	-	-	Caye *et al*., 1968
Ag_2MnSnS_4	Ortho.	$Pmn2_1$ Z= 2	8:1705(5) 6:9413(5) 6:6532(5)	377:33(5)	2.5982)	2.56(2)	2.25(2)	Delgado *et al.*, 2018
	Mon.	*Pc* Z= 2	6.651(1) 6.943(1) 10.536(2) 129.15(1)	377.3(1)	2.933(5)	2.401(4)	2.428(6)	Friedrich *et al*., 2018
Ag_2ZnSiS_4	Mon.	*Pn* Z= 2	6.4052(1) 6.5484(1) 7.9340(1) 90.455(1)	332.77(1)	2.2557(2)	2.344(2)	2.128(4)	Brunetta *et al*., 2012a
Ag_2ZnGeS_4	Tetr.	$I\bar{4}2m$ Z= 2	5.74996(9) 103434(3)	341.98(2)	2.578(5)	2.372(5)	2.332(5)	Parasyuk *et al*., 2010
Ag_2ZnSnS_4	Tetr.	$I\bar{4}$ Z= 2	5.786 10.829	362.53	-	-	-	Johan *et al*., 1982
Ag_2CdGeS_4	Ortho.	$Pmn2_1$ Z= 2	8.0338(3) 6.8680(2) 6.5866(3)	363.43(4)	2.55(1)	2.52(1)	2.22(1)	Parasyuk *et al*., 2005a
	Ortho.	$Pna2_1$ Z= 4	13.7415(8) 8.0367(5) 6.5907(4)	727.85(8	2.558(2)	2.526(2)	2.214(3)	Brunetta *et al*., 2012b
Ag_2CdSnS_4	Ortho.	$Cmc2_1$ Z= 8	4.1015(3) 7.0224(4) 6.6946(4)	192.82(4)	2.478(4)	2.496(5)	2.557(7)	Parasyuk *et al*., 2005b
$Ag_2FeSiSe_4$	Ortho.	$Pmn2_1$	7.653 6.529 6.638	318.79	-	-	-	Quintero *et al*., 1999
$Ag_2FeGeSe_4$	Ortho.	$Pmn2_1$	7.658 6.515 6.434	321.04	-	-	-	Quintero *et al*., 1999
	Ortho.	$Pmn2_1$ Z= 2	7.6478(1) 6.5071(1) 6.4260(1)	319.79(1)	2.450(8)	2.417(8)	2.126(8)	this work
$Ag_2FeSnSe_4$	Ortho.	$Pmn2_1$	7.398 6.993 6.401	331.12	-	-	-	Quintero *et al*., 1999
$Ag_2CdSnSe_4$	Ortho.	$Cmc2_1$ Z= 8	4.2640(2) 7.3170(3) 6.9842(4)	217.6(1)	2.572(2)	2.627(4)	2.649(3)	Parasyuk *et al*., 2002
$Ag_2FeSiTe_4$	Ortho.	$Pmn2_1$	7.721 6.657 6.588	338.65	-	-	-	Quintero *et al*., 1999
$Ag_2FeGeTe_4$	Ortho.	$Pmn2_1$	8.048 6.668 6.450	346.15	-	-	-	Quintero *et al*., 1999
$Ag_2FeSnTe_4$	Ortho.	$Pmn2_1$	8.098 6.785 6.335	348.05	-	-	-	Quintero *et al*., 1999

Mon.= monoclinic, Ortho.= orthorhombic, Tetr.= tetragonal

***Table 2**. SEM experimental results for the sample $Ag_2FeGeSe_4$.*

Composition	MW (g/mol)	Nominal Stoichiometry (%)	Experimental Stoichiometry (%)
$Ag_2FeGeSe_4$	660.03	Ag = 25.0 Fe = 12.5 Ge = 12.5 Se = 50.0	Ag = 25.1 ± 0.2 Fe = 11.2 ± 0.2 Ge = 11.5 ± 0.2 Se = 52.2 ± 0.4

***Table 3.** Results of the Rietveld refinement for $Ag_2FeGeSe_4$.*

Molecular formula	$Ag_2FeGeSe_4$	D_{calc} (g.cm^{-3})	6.85
Molecular weight (g/mol)	660.03 (g/mol)	N° step intensities	4001
a (Å)	7.6478(1)	independent refl.	145
b (Å)	6.5071(1)	Peak-shape profile	Pseudo-Voigt
c (Å)	6.4260(1)		
V (Å^3)	319.79(1)	R_{exp}	6.6 %
System	Orthorhombic	R_p	7.7 %
Space group	*Pmn2$_1$* (N° 31)	R_{wp}	8.4 %
Z	2	S	1.3

$R_p = 100\ \sum|y_{obs} - y_{calc}| / \sum|y_{obs}|$ $\quad R_B = 100\ \sum_k|I_k - Ic_k| / \sum_k |I_k|$ $\quad S = [R_{wp} / R_{exp}]$

$R_{wp} = 100\ [\sum_w|y_{obs} - y_{calc}|^2 / \sum_w|y_{obs}|^2]^{1/2}$ $\quad R_{exp} = 100[(N+C)/\sum_w(y_{obs}^2)]^{1/2}$ $\quad$ N-P+C= degrees of freedom

***Table 4.** Atomic coordinates, occupancy factors and isotropic temperature factor for $Ag_2FeGeSe_4$.*

Atom	Ox.	Wyck.	*x*	*y*	*z*	foc	B (Å^2)
Ag	+1	4*b*	0.255(1)	0.317(1)	0	1	0.51(5)
Fe	+2	2*a*	0	0.849(1)	0.987(1)	1	0.51(5)
Ge	+4	2*a*	0	0.186(1)	0.490(1)	1	0.51(5)
Se1	-2	4*b*	0.237(1)	0.324(1)	0.387(1)	1	0.51(5)
Se2	-2	2*a*	0	0.186(1)	0.822(1)	1	0.51(5)
Se3	-2	2*a*	0	0.885(1)	0.366(1)	1	0.51(5)

***Table 5.** Distance lengths (Å) and bond angles (º) for $Ag_2FeGeSe_4$.*

Ag-Se1	2.491(6)	Fe-Se1^{iv}	2.393(8)	Ge-Se1	2.128(8)
Ag-Se1^{i}	2.447(9)	Fe-Se1^{vi}	2.393(8)	Ge-Se1^{vii}	2.128(8)
Ag-Se2^{ii}	2.416(8)	Fe-Se2^{v}	2.436(9)	Ge-Se2	2.133(9)
Ag-Se3^{i}	2.445(8)	Fe-Se3^{iii}	2.447(9)	Ge-Se3^{viii}	2.115(9)
Se1-Ag-Se2^{ii}	115.8(2)	Se3^{iii}-Fe-Se1^{iv}	108.2(2)	Se1^{vii}-Ge-Se2	108.1(2)
Se1-Ag-Se3^{i}	113.8(2)	Se3^{iii}-Fe-Se1^{vi}	108.2(2)	Se1^{vii}-Ge-Se3^{viii}	105.9(2)
Se1-Ag-Se1^{i}	106.3(2)	Se3^{iii}-Fe-Se2^{v}	110.3(3)	Se1^{vii}-Ge-Se1	116.8(3)
Se1^{i}-Ag-Se3^{i}	112.9(2)	Se2^{v}-Fe-Se1^{iv}	107.9(2)	Se2-Ge-Se3^{viii}	112.1(4)
Se1^{i}-Ag-Se2^{ii}	102.5(2)	Se2^{v}-Fe-Se1^{vi}	107.9(2)	Se2-Ge-Se1	108.1(2)
Se2^{ii}-Ag-Se3^{i}	105.2(2)	Se1^{iv}-Fe-Se1^{vi}	114.4(3)	Se3^{viii}-Ge-Se1	105.9(2)

Symmetry codes: (i) 0.5-x, 1-y, -0.5+z; (ii) x, y, -1+z; (iii) x, y, 1+z; (iv) -0.5+x, 1-y, 0.5+z; (v) x, 1+y, z; (vi) 0.5-x, 1-y, 0.5+z; (vii) -x, y, z; (viii) x, -1+y, z.